2023 Volume 4, Issue 2: 47-64

DOI: https://doi.org/10.48185/jaai.v4i2.920

Simulation modeling with memory-type control charts for monitoring the process variability

Kashinath Chatterjee¹, Mustapha Hached², Christos Koukouvinos³, Angeliki Lappa^{3,*}

¹Department of Population Health Sciences, Division of Biostatistics and Data Science, Augusta University, Augusta, GA 30912-4900

Received: 27.10.2023 • Accepted: 26.12.2023 • Published: 29.12.2023 • Final Version: 29.12.2023

Abstract: Memory-type control charts, renowned for their effectiveness in identifying small deviations in the process variance, are commonly used to monitor the process variability. In this article, we introduce a new tool, the Quadruple Exponentially Weighted Moving Average (QEWMA) chart, which is designed for the specific purpose of monitoring changes in the process variability. We refer to this chart as the S²-QEWMA chart. The performance of the S²-QEWMA chart is assessed through an extensive series of Monte-Carlo simulations, carefully considering the run-length distribution. Comparing it with other well-known memory-type charts, it becomes evident that the S²-QEWMA chart excels in its ability to effectively detect small shifts in the process dispersion. To illustrate the practical application of this chart, we provide an example.

Keywords: average run-length, exponentially weighted moving average, dispersion control chart, Monte-Carlo simulations, standard deviation of run-length.

1. Introduction

In Statistical Process Control (SPC), two types of variations exist within a production process: common causes and assignable causes. A production process is considered to be in statistical control (IC) when it is influenced solely by common causes of variation. Conversely, when assignable causes of variation stem from external sources, they result in a process going out of statistical control (OOC). Control charts play a pivotal role in SPC by detecting assignable causes of variation that can impact process parameters, specifically the mean or variance of the process. These charts can be categorized into two types: location charts, which are effective at identifying deviations in the process mean, and dispersion charts, which are well-suited for detecting variations in process dispersion.

Shewhart-type control charts primarily rely on the most recent observations, making them effective at detecting large shifts in process parameters. Conversely, memory-type control charts, such as the cumulative sum (CUSUM) chart [1, 2] and the exponentially weighted moving average (EWMA) chart [3], take into account both current and past data, rendering them more sensitive in identifying small to moderate shifts. Additionally, innovations have been introduced in this field. Shamma and Shamma [4] and Zhang and Chen [5] developed the Double EWMA (DEWMA) chart,

_

²University of Lille, CNRS, UMR 8524|Laboratoire Paul Painlevé, F-59000 Lille, France

³Department of Mathematics, National Technical University of Athens, Zografou, 15773, Athens, Greece

^{*} Corresponding Author: lappa.angeliki@gmail.com

while Sheu and Lin [6] extended the EWMA chart to create the generally weighted moving average (GWMA) chart. Haq [7, 8] proposed the Hybrid EWMA (HEWMA) chart, and Alevizakos, Chatterjee, and Koukouvinos [9, 10] introduced the Triple EWMA (TEWMA) and Quadruple EWMA (QEWMA) charts for monitoring the process mean.

In many industrial applications, it is crucial to monitor the existence of shifts in the process dispersion rather than the process mean. Therefore, numerous memory-type dispersion control charts have been introduced by prominent scholars. Take for example, Castagliola [11] and Castagliola, Celano and Fichera [12], utilized a three-parameter logarithmic transformation to sample variance (S²) for the purpose of constructing the EWMA and CUSUM charts, namely the S²-EWMA and S²-CUSUM charts. Several authors have also utilized this logarithmic transformation to propose control charts for monitoring the process variability as well. Abbas, Riaz and Does [13] recommended the CS-EWMA chart, Tariq et al. [14] presented the S²-HEWMA chart, Chatterjee, Koukouvinos and Lappa [15] introduced the S²-TEWMA chart, while Alevizakos et al. [16, 17] developed the S²-GWMA and S²-Double GWMA (S²-DGWMA) charts for monitoring the process variability. Additionally, a multitude of dispersion control charts have been introduced in the literature. These include the works of Reynolds and Stoumbos [18], Castagliola et al. [19], Castagliola, Celano and Fichera [20], Shu and Jiang [21], Abbasi et al. [22], Zaman et al. [23], Zhou, Zhou and Geng [24], Sanusi et al. [25], Ali and Haq [26, 27], Haq [28, 29], Abbas et al. [30], Huang, Lu and Chen [31], Riaz et al. [32], Mahadik, Godase and Teoh [33], Arshad, Noor-ul-Amin and Hanif [34], Haq and Razzaq [35], Godase et al. [36], Ajibade et al. [37], Yang, Chen and Lin [38] and Jafari, Maleki and Salmasnia [39].

In this current article, inspired by the research of Castagliola [11] and Alevizakos, Chatterjee, and Koukouvinos [10], we introduce a novel control chart for monitoring process dispersion. This chart is based on a 3-parameter logarithmic transformation to S² and is referred to as the S²-QEWMA chart. To assess its effectiveness, we conduct a comparative study with other control charts, including the S²-EWMA, S²-CUSUM, CS-EWMA, S²-HEWMA, S²-TEWMA, S²-GWMA, and S²-DGWMA charts, using asymptotic control limits. To evaluate these control charts, we employ several Monte-Carlo simulations and consider well-established performance measures such as the average runlength (ARL) and the standard deviation of the run-length (SDRL). These comparisons reveal the efficiency of the proposed memory-type chart in detecting minor shifts in process variability.

The remainder of this article is organized as follows: In Section 2, we will develop the S²-QEWMA chart. In Section 3, we will examine the performance of this newly developed chart. Following that, in Section 4, we will compare its performance with the previously mentioned memory-type dispersion charts using measures like the ARL and the SDRL. Section 5 will provide an illustrative example to explain how to implement the S²-QEWMA chart. Concluding remarks will be summarized in Section 6, and additional technical details of the S²-QEWMA chart can be found in the Appendix.

2. The proposed S²-OEWMA control chart

Consider a sample (or a subgroup) X_{k1}, \ldots, X_{kn} , of n(>1) independent normal distributed $N(\mu_0, \tau\sigma_0)$ random variables, where μ_0 and σ_0 are assumed to be the IC process mean and standard deviation, respectively. Here, k represents the sample number, with k taking on values of 1, 2, If $\tau = 1$, then the process is considered to be IC, whereas the process is declared as OOC when $\tau \neq 1$. Our objective is to promptly detect a shift in the process dispersion, from the IC σ_0^2 value to the OOC $\sigma_1^2 = (\tau\sigma_0)^2$, where $\tau \neq 1$, while ensuring that the process mean remains at its IC value (μ_0) .

$$T_k = a + b \ln(S_k^2 + c)$$
, for $k = 1, 2, ...$ (1)

where $a=A(n)-2B(n)ln(\sigma_0),\ b=B(n),\ c=C(n)\sigma_0^2,\ S_k^2=\frac{1}{n-1}\sum_{j=1}^n\bigl(X_{kj}-\overline{X}_k\bigr)^2$ is the sample variance and $\overline{X}_k=\frac{1}{n}\sum_{j=1}^nX_{kj}$ is the sample mean. According to Castagliola [11], the proper selection of the a, b, and c, implies that the statistic $T_k\approx N(\mu_T(n),\sigma_T^2(n))$. Table 1 provides the values of $A(n),B(n),C(n),\ \mu_T(n)$ and $\sigma_T(n)$ for sample size $n\in\{3,4,\ldots,15\}$, that originally presented in Table I of Castagliola [11].

				- 0	-	
n	A(n)	B(n)	C(n)	$\mu_{T}(n)$	$\sigma_{T}(n)$	Q_0
3	-0.6627	1.8136	0.6777	0.02472	0.9165	0.276
4	-0.7882	2.1089	0.6261	0.01266	0.9502	0.237
5	-0.8969	2.3647	0.5979	0.00748	0.9670	0.211
6	-0.9940	2.5941	0.5801	0.00485	0.9765	0.193
7	-1.0827	2.8042	0.5678	0.00335	0.9825	0.178
8	-1.1647	2.9992	0.5588	0.00243	0.9864	0.167
9	-1.2413	3.1820	0.5519	0.00182	0.9892	0.157
10	-1.3135	3.3548	0.5465	0.00141	0.9912	0.149
11	-1.3820	3.5189	0.5421	0.00112	0.9927	0.142
12	-1.4473	3.6757	0.5384	0.00090	0.9938	0.136
13	-1.5097	3.8260	0.5354	0.00074	0.9947	0.131
14	-1.5697	3.9705	0.5327	0.00062	0.9955	0.126
15	-1.6275	4.1100	0.5305	0.00052	0.9960	0.122

Table 1. Values of A(n), B(n), C(n), $\mu_T(n)$, $\sigma_T(n)$ and Q₀ for sample size $n \in \{3, 4, ..., 15\}$

The plotting statistic Q_k of the $\,S^2\text{-}QEWMA$ control chart for monitoring the process variability is given by

$$Z_{k} = \lambda T_{k} + (1 - \lambda) Z_{k-1}$$

$$Y_{k} = \lambda Z_{k} + (1 - \lambda) Y_{k-1}$$

$$W_{k} = \lambda Y_{k} + (1 - \lambda) W_{k-1}$$

$$Q_{k} = \lambda W_{k} + (1 - \lambda) Q_{k-1}$$
for $k = 1, 2, ...$
(2)

where λ is the smoothing parameter with $0 < \lambda \le 1$, and $Q_0 = W_0 = Y_0 = Z_0 = A(n) + B(n)\ln(1 + C(n))$ are the starting values. The Q_0 values are also provided in Table 1 for $n \in \{3, 4, ..., 15\}$.

The mean of the statistic Q_k is given by

$$E(Q_k) = \mu_T(n). \tag{3}$$

The variance of the statistic Q_k is defined as

$$Var(Q_k) = V(d, k)\sigma_T^2(n)$$
(4)

where V(d, k) is given by

$$V(d,k) = \frac{\lambda^8}{36} \left[-\left[k(k^2 - 1)(k - 2)(k - 3)(k - 4) + 21k(k^2 - 1)(k - 2)(k - 3) + 138k(k^2 - 1)(k - 2) + 330k(k^2 - 1) + 252k(k + 1) + 36(k + 1) \right] \frac{d^k}{1 - d}$$

$$-\left[6k(k^{2}-1)(k-2)(k-3)+105k(k^{2}-1)(k-2)+552k(k^{2}-1)+990k(k+1)\right.\\ \left.+504(k+1)+36\right]\frac{d^{k+1}}{(1-d)^{2}}\\ -\left[30k(k^{2}-1)(k-2)+420k(k^{2}-1)+1656k(k+1)+1908(k+1)+504\right]\frac{d^{k+2}}{(1-d)^{3}}\\ -\left[120k(k^{2}-1)+1260k(k+1)+3312(k+1)+1980\right]\frac{d^{k+3}}{(1-d)^{4}}\\ -\left[360k(k+1)+2520(k+1)+3312\right]\frac{d^{k+4}}{(1-d)^{5}}-\left[720(k+1)+2520\right]\frac{d^{k+5}}{(1-d)^{6}}\\ -720\frac{d^{k+6}}{(1-d)^{7}}+\left[\frac{720d^{5}}{(1-d)^{7}}+\frac{2520d^{4}}{(1-d)^{6}}+\frac{3312d^{3}}{(1-d)^{5}}+\frac{1980d^{2}}{(1-d)^{4}}+\frac{504d}{(1-d)^{3}}+\frac{36}{(1-d)^{2}}\right].$$

and $d = (1 - \lambda)^2$. For large values of $k (k \to \infty)$, the asymptotic variance of the statistic Q_k becomes

$$Var(Q_k) = V(d, \infty)\sigma_T^2(n). \tag{6}$$

where

$$V(d,k\to\infty) = \frac{\lambda^8}{36} \left[\frac{720d^5}{(1-d)^7} + \frac{2520d^4}{(1-d)^6} + \frac{3312d^3}{(1-d)^5} + \frac{1980d^2}{(1-d)^4} + \frac{504d}{(1-d)^3} + \frac{36}{(1-d)^2} \right]. \tag{7}$$

The derivation of the mean and the variance of the statistic Q_k is provided in the Appendix in detail.

Consequently, the control limits of the S²-QEWMA chart are given by

$$\begin{split} LCL_k &= \mu_T(n) - L\sqrt{V(Q)} \\ CL_k &= \mu_T(n) \\ UCL_k &= \mu_T(n) + L\sqrt{V(Q)}, \end{split} \tag{8}$$

with L >0 being the control chart multiplier. For simplicity purposes, the asymptotic control limits are used for the construction of the S^2 -QEWMA control chart, by computing the variance of the statistic Q_k given in Eq. (6). The S^2 -QEWMA chart is designed by plotting the statistic Q_k versus the subgroup number k. The process is considered to be OOC when $Q_k \leq LCL_k$ or $Q_k \geq UCL_k$; otherwise, it is said to be IC.

3. Performance evaluation of the S² -QEWMA chart

In the current section, we examine the efficiency of the S^2 -QEWMA chart. Traditionally, the statistical performance of a control chart is measured using the ARL, the SDRL and the percentile points. Particularly, the ARL is described as the average number of statistics that must be plotted on a chart until an OOC signal is raised. When the process variability is IC ($\tau = \sigma_1/\sigma_0 = 1$), a large value of IC ARL (ARL₀) is suggested to avoid false alarms. Nevertheless, when the process is OOC, i.e. $\tau \neq 1$, a small OOC ARL (ARL₁) value is preferable so as to detect the shift in the process variability quickly. Here, both the ARL and SDRL measures are used to examine the performance of the S^2 -QEWMA control chart.

The run-length distribution of the proposed S²-QEWMA chart is evaluated via a Monte-Carlo simulation algorithm using the R statistical software. The algorithm is run 10000 iterations, so as to calculate the mean and the standard deviation of the 10000 run-lengths. We assume that the

process for the IC state is normally distributed with $\mu_0=0$ and $\sigma_1=\tau\sigma_0$ ($\tau=1.00$), whereas the OOC process follows the Normal distribution with mean $\mu_1=0$ and standard deviation $\sigma_1=\tau\sigma_0$ ($\tau\neq1.00$). Furthermore, the statistical design of the S^2 -QEWMA chart requires the finding of the (λ,L) design parameter combinations, in order to achieve a pre-fixed ARL $_0$ value for a specified value of the sample size n. Consequently, the L values are obtained via Monte-Carlo simulations considering the asymptotic control limits of the S^2 -QEWMA chart given in Eq. (8), by calculating the asymptotic variance of statistic Q_k given in Eq. (6), for various λ and n values when ARL $_0\approx200$, 370 and 500.

Table 2 provides the (λ, L) design parameter combinations of the S^2 -QEWMA control chart with $\lambda \in \{0.10, 0.15, \ldots, 0.95, 1.00\}$, when $n \in \{3, 5, 7, 9\}$ and $ARL_0 \approx 200, 370$ and 500. Tables A1 and A2 in the Supplementary Material present the ARL and the SDRL (in the parenthesis) results of the S^2 -QEWMA control chart with $\lambda \in \{0.10, 0.15, 0.20, 0.25, 0.30, 0.35, 0.40, 0.50\}$ using asymptotic control limits, when $n \in \{5, 9\}$ as well as $ARL_0 \approx 200$ and 370. It is to be noted that, the dispersion shifts between σ_0 and $\sigma_1 = \tau \sigma_0$, where $\tau = \frac{\sigma_1}{\sigma_0} \in \{0.50, 0.60, 0.70, 0.80, 0.90, 0.95, 1.00, 1.05, 1.10, 1.20, 1.30, 1.40, 1.50, 1.60, 1.70, 1.80, 1.90, 2.00\}$. In case of $\tau < 1.00$, we refer to downward shifts, whereas $\tau > 1.00$ is related with the upward shifts. The smallest ARL_1 values are indicated with bold print for each shift τ in Tables A1 and A2 in the Supplementary Material as well.

Table 2. (λ , L) parameter combinations for the S²-QEWMA control chart when $n \in \{3, 5, 7, 9\}$ and, $ARL_0 \approx 200, 370$ and 500

	AR	$L_0 \approx 200$	1			37	70		500			
λ	n =3	5	7	9	3	5	7	9	3	5	7	9
0.10	2.1354	1.6908	1.6140	1.5830	2.1364	1.9165	1.9053	1.8839	2.1551	2.0432	2.0355	2.0250
0.15	1.8600	1.8110	1.7975	1.7840	2.1069	2.0890	2.0832	2.0800	2.2334	2.2225	2.2185	2.2165
0.20	1.9630	1.9550	1.9445	1.9410	2.2275	2.2255	2.2272	2.2256	2.3555	2.3542	2.3520	2.3520
0.25	2.0682	2.0712	2.0655	2.0600	2.3330	2.3325	2.3340	2.3300	2.4531	2.4538	2.4535	2.4520
0.30	2.1556	2.1610	2.1608	2.1590	2.4160	2.4186	2.4180	2.4148	2.5300	2.5360	2.5365	2.5346
0.35	2.2350	2.2110	2.2450	2.2450	2.4860	2.4930	2.4912	2.4930	2.6000	2.6040	2.6040	2.6080
0.40	2.3025	2.3135	2.3200	2.3150	2.5460	2.5565	2.5540	2.5605	2.6600	2.6670	2.6625	2.6723
0.50	2.4222	2.4310	2.4376	2.4410	2.6520	2.6550	2.6640	2.6685	2.7640	2.7580	2.7690	2.7782
0.60	2.5170	2.5300	2.5350	2.5500	2.7475	2.7400	2.7515	2.7620	2.8565	2.8390	2.8486	2.8605
0.70	2.6084	2.6089	2.6198	2.6340	2.8500	2.8062	2.8209	2.8350	2.9640	2.8975	2.9179	2.9270
0.75	2.6560	2.6318	2.6500	2.6650	2.9010	2.8250	2.8445	2.8550	3.0125	2.9190	2.9346	2.9470
0.80	2.7050	2.6445	2.6700	2.6850	2.9455	2.8342	2.8530	2.8710	3.0560	2.9240	2.9405	2.9568
0.90	2.7700	2.6330	2.6489	2.6740	2.9820	2.8275	2.8205	2.8420	3.0785	2.9200	2.9033	2.9200
0.95	2.7825	2.6345	2.6170	2.6530	2.9790	2.8275	2.7905	2.8120	3.0695	2.9166	2.8736	2.8905
1.00	2.7910	2.6384	2.5990	2.6370	2.9810	2.8280	2.7855	2.7940	3.0692	2.9135	2.8750	2.8725

The results in Tables A1 and A2 in the Supplementary Material reveal that:

- Small λ values are preferable for detecting moderate downward to small upward shifts (0.80 \leq $\tau \leq$ 1.20) in the variability.
- Large values of λ are recommended for detecting large downward ($\tau < 0.80$) and moderate to large upward ($\tau > 1.20$) shifts in the variability.
- As the ARL₀ decreases, both the ARL₁ and SDRL₁ decrease for all the examined τ and n values.
- Generally, the efficiency of the S²-QEWMA chart improves, as the sample size n increases. However, the opposite happens for the ARL measure at i) $\lambda = 0.10$ and $\tau \ge 1.20$ when ARL₀ \approx

200, ii) $\lambda=0.10$ and $\tau\geq 1.30$ when $ARL_0\approx 370$, iii) $\lambda=0.15$ and $\tau\geq 1.70$ when $ARL_0\approx 200$, as well as iv) $\lambda=0.15$ and $\tau=2.00$ when $ARL_0\approx 370$.

- The SDRL₀ decreases as the n value increments for the majority of the examined scenarios, except for the cases that $\lambda = 0.25, 0.30$ and 0.40 when ARL₀ ≈ 200 .
- Both ARL₁ and SDRL₁ decrease, as the τ value increases or decreases for the examined λ cases.
- The S²-QEWMA chart is more sensitive in detecting the upward shifts than the downward shifts in the variability. For instance, when $ARL_0 \approx 370$ and n=5, the ARL_1 values of the S²-QEWMA control chart with $\lambda=0.10,0.20$ and 0.30, at $\tau=0.90$, are 78.08, 82.17 and 101.20, respectively, whereas the corresponding ARL_1 values at $\tau=1.10$ are 48.85, 63.86, and 71.19. Nevertheless, the results show that the proposed chart with $\lambda=0.50$ is less efficient in detecting large upward shifts than large downward shifts in the variability.

4. Performance comparisons

Here, we compare the performance of the S^2 -QEWMA chart with that of some recently developed memory-type control charts in the literature, such as the S^2 -GWMA, S^2 -EWMA, S^2 -CUSUM, CS-EWMA, S^2 -HEWMA, S^2 -TEWMA and S^2 -DGWMA charts. We use run length measures, like the ARL and the SDRL. For a pre-fixed ARL₀ value, the control chart with the smaller ARL₁ value can detect the shift faster compared with the other competing control charts. Consequently, in order to have fair comparisons, we take into consideration these control charts assuming two-sided asymptotic control limits, ARL₀ \approx 370 as well as n = 5. Tables A3 to A8 in the Supplementary Material present the ARL and SDRL (in the parenthesis) results of these charts, for the same τ values $(0.50 \le \tau \le 2.00)$ as in Section 3. Note that the design parameters of the S^2 -GWMA, S^2 -EWMA, S^2 -CUSUM, CS-EWMA, S^2 -HEWMA, S^2 -TEWMA and S^2 -DGWMA charts are obtained through Monte-Carlo simulations such that ARL₀ \approx 370 and n = 5. The considered control charts are briefly described, and compared individually with the proposed S^2 -QEWMA chart.

• S²-QEWMA chart versus S²-GWMA chart

The plotting statistic of the S²-GWMA chart is given by

$$G_k = \sum_{j=1}^k \! \left(q^{(j-1)^\alpha} - q^{j^\alpha} \right) \! T_{k-j+1} + q^{k^\alpha} G_0 \text{, for } k = 1,\!2, ... \tag{9}$$

with the statistic T_k being given by the Eq. (1), $q \in [0,1)$ being the design parameter, $\alpha > 0$ being the adjustment parameter and $G_0 = Q_0$ being the starting value. The asymptotic control limits of the S^2 -GWMA chart are given by

$$\begin{aligned} \text{LCL} &= \mu_{T}(n) - \text{L}\sigma_{T}(n)\sqrt{D} \\ \text{CL} &= \mu_{T}(n) \end{aligned} \tag{10} \\ \text{UCL} &= \mu_{T}(n) + \text{L}\sigma_{T}(n)\sqrt{D} \end{aligned}$$

where L(>0) is the control chart multiplier, $D = \lim_{k \to \infty} D_k$ and $D_k = \sum_{j=1}^k (q^{(j-1)^\alpha} - q^{j^\alpha})^2$, k = 1, 2, ... It is also worth mentioning that, the S²-GWMA chart reduces to the S²-EWMA chart when $q = 1 - \lambda$ and $\alpha = 1.00$, where $\lambda \in (0.00, 1.00]$ is the smoothing parameter of the latter chart. In order to construct the S²-GWMA chart, we plot, the statistic G_k versus the sample number k. The process is declared as OOC, when $G_k \le LCL$ or $G_k \ge UCL$; otherwise the process is considered to be IC. Table A3 in the Supplementary Material presents the ARL and SDRL (in the parenthesis) values of the S²-GWMA chart for various (q, α, L) combinations when $ARL_0 \approx 370$ and n = 5.

According to Tables A2 and A3 in the Supplementary Material, the proposed chart is more efficient than the S²-GWMA chart in detecting small downward to small upward shifts. For instance,

• S²-QEWMA chart versus S²-CUSUM chart

The plotting statistics of the S²-CUSUM chart are given by

$$C_{k}^{-} = \max[0, C_{k-1}^{-} + \mu_{T}(n) - T_{k} - K]$$

$$C_{k}^{+} = \max[0, C_{k-1}^{+} + T_{k} - \mu_{T}(n) - K]'$$
 for $k = 1, 2, ...$ (11)

where the statistic T_k is given by Eq. (1), $K(\ge 0)$ is the reference value and $C_0^- = C_0^+ = 0$ are the starting values. The C_k^- and C_k^+ statistics are plotted against the decision interval H. The process is declared as OOC, if either of the two statistics is plotted above $H(\ge 0)$. Table A4 in the Supplementary Material presents the ARL and SDRL (in the parenthesis) results of the S²-CUSUM chart for various (K, H) combinations when $ARL_0 \approx 370$ and n = 5.

Tables A2 and A4 in the Supplementary Material indicate that the S^2 -QEWMA chart is more efficient than the S^2 -CUSUM chart in identifying large downward to small upward shifts in the variability. For example, the S^2 -QEWMA chart with $\lambda \in \{0.15, 0.20, 0.25\}$ is more effective than the S^2 -CUSUM chart with K = 0.50 at $0.80 \le \tau \le 1.20$. Furthermore, the S^2 -QEWMA chart with $\lambda = 0.25$ is better than the S^2 -CUSUM chart with K = 1.00 at $0.60 \le \tau \le 1.20$, and the S^2 -QEWMA chart with $\lambda = 0.40$ is more efficient than the S^2 -CUSUM chart with K = 1.25 at $0.50 \le \tau < 1.00$ as well as $1.10 \le \tau \le 1.30$. Nevertheless, the opposite is observed for the ARL measure in case of moderate to large upward shifts. For instance, the S^2 -CUSUM chart with K = 0.50 has lower ARL₁ values than the S^2 -QEWMA chart with K = 0.50 has lower ARL₂ performance of the K = 0.50 has lower than that of the K = 0.50 has lower of the examined cases.

• S²-QEWMA chart versus CS-EWMA chart

The charting statistics of the CS-EWMA chart are defined as

$$\begin{split} M_k^- &= \text{max}[0, M_{k-1}^- + \mu_T(n) - Z_k - K'] \\ M_k^+ &= \text{max}[0, M_{k-1}^+ + Z_k - \mu_T(n) - K']' \end{split} \text{ for } k = 1, 2, ... \end{split} \tag{12}$$

where $Z_k = \lambda T_k + (1-\lambda)Z_{k-1}$ for k=1,2,..., $\lambda \in (0,1]$ is the smoothing parameter, $M_0^- = M_0^+ = 0$ are the starting values, and $K' = K_{CS}\sqrt{\frac{\lambda}{2-\lambda}}$ is the reference value with $K_{CS} \geq 0$. The statistics M_k^- and M_k^+ are plotted against the decision interval $H' = H_{CS}\sqrt{\frac{\lambda}{2-\lambda}}$, while the process raises an OOC signal if either M_k^- or M_k^+ is plotted over the H'. The ARL and the SDRL (in the parenthesis) values for the CS-EWMA chart are displayed in Table A5 in the Supplementary Material for various $(\lambda, K_{CS}, H_{CS})$ combinations when ARL $_0 \approx 370$ and n=5.

Tables A2 and A5 in the Supplementary Material reveal that the proposed chart has lower ARL₁ values compared with the CS-EWMA chart in detecting small shifts. For instance, the S²-QEWMA ($\lambda \in \{0.15, 0.20, 0.25\}$) chart is more sensitive than the CS-EWMA ($\lambda \in \{0.15, 0.20, 0.25\}$, $K_{CS} = 1.00$) chart at $0.90 \le \tau \le 1.10$, the S²-QEWMA ($\lambda = 0.30$) chart is better than the CS-EWMA ($\lambda = 0.30$, $K_{CS} = 1.00$) chart at $0.90 \le \tau < 1.00$ and $\tau = 1.10$, and the S²-QEWMA ($\lambda \in \{0.35, 0.40, 0.50\}$) is more efficient than the CS-EWMA ($\lambda \in \{0.35, 0.40, 0.50\}$), $K_{CS} = 1.00$) chart at $0.90 \le \tau < 1.00$, while the opposite is observed for the remaining τ values. It should be pointed out that, the S²-QEWMA ($\lambda \in \{0.15, 0.20, 0.25\}$) chart has better SDRL performance compared with that of the CS-EWMA ($\lambda \in \{0.15, 0.20, 0.25\}$), $K_{CS} = 1.00$) chart for most of the considered τ values. As λ increases, the S²-QEWMA chart has lower SDRL₁ values than the CS-EWMA chart for downward, as well as moderate to large upward shifts in the variability. For example, the S²-QEWMA ($\lambda = 0.35$) chart has lower SDRL₁ results than the CS-EWMA ($\lambda = 0.35$, $K_{CS} = 1.00$) chart at $0.50 \le \tau < 1.00$ and $1.30 \le \tau \le 2.00$.

• S²-OEWMA chart versus S²-HEWMA chart

The plotting statistic Y_k of the S²-HEWMA chart is given through the following system of equations

$$Y_k = \lambda_1 Z_k + (1 - \lambda_1) Y_{k-1}
Z_k = \lambda_2 T_k + (1 - \lambda_2) Z_{k-1}$$
 for $k = 1, 2, ...$ (13)

where T_k is given by Eq. (1), $\lambda_1, \lambda_2 \in (0, 1]$ are the smoothing parameters, and $Y_0 = Z_0 = Q_0$ are the starting values. Given $\lambda_1 \neq \lambda_2$, the asymptotic control limits of the S^2 -HEWMA chart are given by

$$\begin{split} LCL &= \mu_T(n) - L\sigma_T(n) \left(\frac{\lambda_1 \lambda_2}{\lambda_1 - \lambda_2}\right) \sqrt{\sum_{i=1}^2 \frac{(1 - \lambda_i)^2}{1 - (1 - \lambda_i)^2} - \frac{2(1 - \lambda_1)(1 - \lambda_2)}{1 - (1 - \lambda_1)(1 - \lambda_2)}} \\ &\qquad \qquad CL = \mu_T(n) \\ UCL &= \mu_T(n) + L\sigma_T(n) \left(\frac{\lambda_1 \lambda_2}{\lambda_1 - \lambda_2}\right) \sqrt{\sum_{i=1}^2 \frac{(1 - \lambda_i)^2}{1 - (1 - \lambda_i)^2} - \frac{2(1 - \lambda_1)(1 - \lambda_2)}{1 - (1 - \lambda_1)(1 - \lambda_2)}} \end{split}$$

where L(> 0) is the control chart multiplier. When $\lambda_1 = \lambda_2$, the asymptotic control limits of the S²-HEWMA chart are given by

$$\begin{split} LCL &= \mu_T(n) - L\sigma_T(n) \sqrt{\frac{\lambda(2-2\lambda+\lambda^2)}{(2-\lambda)^3}} \\ &CL = \mu_T(n) \\ UCL &= \mu_T(n) + L\sigma_T(n) \sqrt{\frac{\lambda(2-2\lambda+\lambda^2)}{(2-\lambda)^3}} \end{split} \tag{15}$$

The S^2 -HEWMA control chart is designed by plotting the statistic Y_k versus the subgroup number k. The process is considered to be IC, if $LCL < Y_k < UCL$. Table A6 in the Supplementary Material

The comparison of the results between Tables A2 and A6 in the Supplementary Material indicates that the proposed chart is better than the S^2 -HEWMA chart in detecting small deviations in the process dispersion. Particularly, as the λ value increases, the ARL performance of the S^2 -QEWMA chart improves in detecting moderate to large downward shifts compared with the competing chart. Additionally, the proposed chart has better SDRL performance than that of the S^2 -HEWMA chart for most of the examined cases and τ values. For example, the S^2 -QEWMA ($\lambda = 0.15$) chart has lower ARL₁ values at $0.90 \le \tau \le 1.10$, as well as lower SDRL₁ values at $0.50 \le \tau \le 2.00$, in comparison with the S^2 -HEWMA ($\lambda_1 = 0.15, \lambda_2 \in \{0.15, 0.20, 0.25, 0.30, 0.35, 0.40, 0.50\}$) chart. Furthermore, comparing the S^2 -QEWMA ($\lambda = 0.35$) and S^2 -HEWMA ($\lambda_1 = 0.35, \lambda_2 \in \{0.35, 0.40, 0.50\}$) charts, we observe that the first chart has better ARL performance at $0.70 \le \tau < 1.00$ and $\tau = 1.10$, as well as better SDRL performance at $0.50 \le \tau < 1.00$ and $1.10 \le \tau \le 2.00$ than the latter chart.

• S²-QEWMA chart versus S²-TEWMA chart

The plotting statistic W_k of the S²-TEWMA chart is given through the following system of equations

$$Z_{k} = \lambda T_{k} + (1 - \lambda) Z_{k-1}$$

$$Y_{k} = \lambda Z_{k} + (1 - \lambda) Y_{k-1}$$

$$W_{k} = \lambda Y_{k} + (1 - \lambda) W_{k-1}$$
for $k = 1, 2, ...$ (16)

where T_k is given by Eq. (1), $\lambda \in (0,1]$ is the smoothing constant, and $W_0 = Y_0 = Z_0 = Q_0$ are the starting values. The asymptotic control limits of the S^2 -TEWMA chart are given by

$$\begin{split} LCL &= \mu_T(n) - L\sigma_T(n) \sqrt{\left[\frac{6(1-\lambda)^6\lambda}{(2-\lambda)^5} + \frac{12(1-\lambda)^4\lambda^2}{(2-\lambda)^4} + \frac{7(1-\lambda)^2\lambda^3}{(2-\lambda)^3} + \frac{\lambda^4}{(2-\lambda)^2}\right]} \\ &\qquad \qquad CL = \mu_T(n) \\ UCL &= \mu_T(n) + L\sigma_T(n) \sqrt{\left[\frac{6(1-\lambda)^6\lambda}{(2-\lambda)^5} + \frac{12(1-\lambda)^4\lambda^2}{(2-\lambda)^4} + \frac{7(1-\lambda)^2\lambda^3}{(2-\lambda)^3} + \frac{\lambda^4}{(2-\lambda)^2}\right]} \end{split} \label{eq:lcl}$$

where L(> 0) is the control chart multiplier. The S²-TEWMA chart is constructed by plotting the statistic W_k versus the sample number k and the process raises an OOC signal, when $W_k \leq$ LCL or $W_k \geq$ UCL. The ARL and SDRL (in the parenthesis) values of the S²-TEWMA chart are presented in Table A7 in the Supplementary Material for various (λ , L) combinations when ARL₀ \approx 370 and n = 5.

Tables A2 and A7 in the Supplementary Material reveal that the S²-QEWMA chart is more sensitive than the S²-TEWMA chart in identifying small upward and downward shifts in the variability. Additionally, as the parameter λ increments, the proposed chart becomes more efficient than the S²-TEWMA chart in detecting moderate to large downward shifts. However, we observe that, the S²-QEWMA chart with $\lambda \in \{0.40, 0.50\}$ is less efficient than the competing chart for small upward shifts. In case of the moderate to large upward shifts, the S²-TEWMA chart shows lower ARL₁ values than the proposed chart. It must be noted that, the S²-QEWMA chart shows better SDRL performance for most of the examined λ and τ values, except e.g when i) $\lambda = 0.10$ at $0.50 \le \tau \le 0.60$, ii) $\lambda = 0.15$ at $1.90 \le \tau \le 2.00$, iii) $\lambda = 0.40$ at $\tau = 1.05$, and iv) $\lambda = 0.50$ at $1.05 \le \tau \le 1.10$. For example, the S²-QEWMA ($\lambda = 0.20$) chart has lower ARL₁ results at $0.90 \le \tau \le 1.10$, while it has lower SDRL₁ results at $0.50 \le \tau \le 2.00$ compared with the S²-TEWMA ($\lambda = 0.20$) chart.

Furthermore, the S²-QEWMA ($\lambda = 0.40$) chart has better ARL performance at $0.70 \le \tau \le 0.95$ and $\tau = 1.10$, as well as better SDRL performance at $0.50 \le \tau \le 0.95$ and $1.05 \le \tau \le 2.00$, compared with the S²-TEWMA ($\lambda = 0.40$) chart.

• S²-QEWMA chart versus S²-DGWMA chart

The plotting statistic of the S²-DGWMA chart is defined through the following system of equations

$$\begin{cases} G_{k} = \sum_{j=1}^{k} (q^{(j-1)^{\alpha}} - q^{j^{\alpha}}) T_{k-j+1} + q^{k^{\alpha}} G_{0} \\ DG_{k} = \sum_{j=1}^{k} (q^{(j-1)^{\alpha}} - q^{j^{\alpha}}) G_{k-j+1} + q^{k^{\alpha}} DG_{0} \end{cases}, \text{ for } k = 1, 2, ...$$
 (18)

where the statistic T_k is given by Eq. (1), $q \in [0, 1)$ is the design parameter, $\alpha > 0$ is the adjustment parameter and $DG_0 = G_0 = Q_0$ are the starting values. The asymptotic control limits of the S^2 -DGWMA chart are given by

$$\begin{split} LCL_k &= \mu_T(n) - L\sigma_T(n)\sqrt{F} \\ CL_k &= \mu_T(n) \\ UCL_k &= \mu_T(n) + L\sigma_T(n)\sqrt{F} \end{split} \tag{19}$$

where $F = \lim_{k \to \infty} F_k$ and $F_k = \sum_{j=1}^k \left(\sum_{u=j}^k \left(q^{(k-u)^\alpha} - q^{(k-u+1)^\alpha} \right) \left(q^{(u-j)^\alpha} - q^{(u-j+1)^\alpha} \right) \right)^2$. The S²-DGWMA chart is designed by plotting the statistic DG_k versus the sample number k. The process is declared as IC, when LCL < DG_k < UCL; otherwise, it is considered to be OOC. It is important to note that, the S²-DGWMA chart reduces to the S²-HEWMA chart when $q = 1 - \lambda$, $\alpha = 1$ and $\lambda = \lambda_1 = \lambda_2$. Table A8 in the Supplementary Material presents the ARL and SDRL (in the parenthesis) values of the S²-DGWMA chart for various (q, α, L) combinations when ARL₀ ≈ 370 and n = 5. It is to be noted that the ARL and SDRL results of the S²-DGWMA $(q = 1 - \lambda, \alpha = 1)$ chart are presented in Table A6 for $\lambda = \lambda_1 = \lambda_2$.

The comparison of the results between Tables A2 and A8 in the Supplementary Material shows that the S²-QEWMA chart is better than the S²-DGWMA chart in detecting small shifts in the process dispersion. Furthermore, as the λ value increments, the ARL performance of the S²-QEWMA chart is better in detecting moderate to large downward shifts in comparison with the competing chart. Additionally, the newly developed chart has better SDRL performance than that of the S²-DGWMA chart for most of the examined scenarios and τ values. For instance, the S²-QEWMA (λ = 0.25) chart has lower ARL₁ values at 0.80 ≤ τ ≤ 1.20 in comparison with the S²-DGWMA (α = 0.75, α = 1.20) chart. Furthermore, the S²-QEWMA (α = 0.30) chart has better SDRL₁ results at τ ≤ 1.00 and τ ≥ 1.40 in comparison with the S²-DGWMA (α = 0.70, α = 0.80) chart.

5. An Illustrative example

In the current example, a simulated dataset is used in order to illustrate the application of the S²-QEWMA control chart. A dataset with 30 samples of size n=5 is generated, in which the X_{kj} , $k=1,2,\ldots,30$, and $j=1,2,\ldots,5$, are mutually independent and follow the $N(\mu_0,\sigma_1=\tau\sigma_0)$. The first 10 samples are generated from $N(\mu_0=15,\sigma_0=1.50)$ ($\tau=1.00$). However, a shift of $\sigma_1=1.10\sigma_0$ ($\tau=1.10$) is added in the standard deviation of the remaining 20 samples. The simulated data, are provided in Table 3.

Table 3. Data and Calculation Details

Sample,	Simulated Data			T_k	S ² -EWMA	S ² -CUSUM		CS-EWMA		S ² -HEWMA	S ² -TEWMA	S ² -GWMA	S ² -QEWMA		
1	18.418	21.277	20.400	17.783	21.501	0.574	0.284	0.000	0.067	0.000	0.000	0.226	0.214	0.284	0.212
2	21.667	21.036	18.114	22.398	20.986	0.461	0.319	0.000	0.020	0.000	0.000	0.244	0.220	0.305	0.213
3	21.877	19.301	20.232	19.997	18.280	-0.142	0.227	0.000	0.000	0.000	0.000	0.241	0.224	0.205	0.215
4	20.605	18.455	20.073	19.103	20.344	-0.988	-0.016	0.496	0.000	0.000	0.000	0.189	0.217	-0.021	0.216
5	19.728	18.197	23.577	19.324	20.847	1.229	0.233	0.000	0.722	0.000	0.000	0.198	0.213	0.277	0.215
6	20.932	19.591	21.396	21.063	17.676	0.281	0.243	0.000	0.495	0.000	0.000	0.207	0.212	0.245	0.215
7	19.080	21.491	17.479	20.389	23.113	1.439	0.482	0.000	1.426	0.000	0.141	0.262	0.222	0.477	0.216
8	20.458	19.154	19.134	18.480	21.690	-0.219	0.342	0.000	0.700	0.000	0.142	0.278	0.233	0.290	0.220
9	22.231	20.185	19.111	18.760	17.934	0.516	0.376	0.000	0.708	0.000	0.177	0.298	0.246	0.346	0.225
10	18.072	21.237	21.660	21.351	19.035	0.430	0.387	0.000	0.631	0.000	0.224	0.316	0.260	0.354	0.232
11	17.495	19.264	21.702	21.226	19.874	0.547	0.419	0.000	0.670	0.000	0.302	0.336	0.275	0.386	0.241
12	22.522	21.382	19.428	20.096	22.055	-0.178	0.300	0.000	0.000	0.000	0.261	0.329	0.286	0.263	0.250
13	20.701	17.096	17.614	20.543	20.869	0.874	0.415	0.000	0.366	0.000	0.335	0.346	0.298	0.402	0.259
14	20.196	18.640	18.591	21.173	18.185	-0.245	0.283	0.000	0.000	0.000	0.277	0.333	0.305	0.253	0.268
15	19.022	19.303	17.344	21.736	22.150	1.160	0.458	0.000	0.652	0.000	0.394	0.358	0.316	0.453	0.278
16	19.450	23.238	20.160	18.333	20.516	0.828	0.532	0.000	0.972	0.000	0.585	0.393	0.331	0.498	0.289
17	22.974	20.602	21.520	17.284	20.762	1.310	0.687	0.000	1.774	0.000	0.932	0.452	0.355	0.638	0.302
18	20.174	20.783	22.052	18.122	20.301	0.052	0.560	0.000	1.319	0.000	1.151	0.474	0.379	0.481	0.317
19	17.094	18.703	18.688	20.574	18.761	-0.326	0.383	0.000	0.485	0.000	1.193	0.455	0.394	0.327	0.333
20	21.483	21.602	17.987	17.478	22.418	1.632	0.633	0.000	1.609	0.000	1.485	0.491	0.414	0.617	0.349
21	20.846	21.254	20.973	21.588	23.930	-0.252	0.456	0.000	0.849	0.000	1.600	0.484	0.428	0.401	0.365
22	19.288	23.245	20.663	16.931	18.980	1.715	0.708	0.000	2.057	0.000	1.967	0.529	0.448	0.685	0.381
23	18.717	22.013	19.200	20.510	21.758	0.165	0.599	0.000	1.715	0.000	2.225	0.543	0.467	0.534	0.398
24	18.591	20.650	19.393	20.554	21.603	-0.442	0.391	0.000	0.765	0.000	2.275	0.512	0.476	0.345	0.414
25	20.227	17.806	21.449	21.948	19.326	0.534	0.419	0.000	0.791	0.000	2.354	0.494	0.480	0.418	0.427
26	20.363	21.230	18.841	17.383	17.204	0.752	0.486	0.000	1.036	0.000	2.499	0.492	0.482	0.487	0.438
27	20.614	19.778	21.529	18.868	21.625	-0.444	0.300	0.000	0.085	0.000	2.459	0.454	0.476	0.290	0.446
28	19.630	20.128	17.273	21.570	20.196	0.340	0.308	0.000	0.000	0.000	2.426	0.425	0.466	0.333	0.450
29	19.868	18.380	19.463	19.516	21.847	-0.259	0.195	0.000	0.000	0.000	2.280	0.379	0.449	0.222	0.450
30	21.086	20.464	21.711	21.643	19.794	-1.166	-0.078	0.674	0.000	0.000	1.861	0.287	0.416	-0.029	0.443

Assuming ARL $_0\approx 370$, we construct the proposed S²-QEWMA ($\lambda=0.20, L=2.2255$) chart, along with the S²-EWMA ($\lambda=0.20, L=2.8004$) (i.e. S²-GWMA ($q=0.80, \alpha=1.00, L=2.8004$)), S²-CUSUM (K = 0.50, H = 4.412), CS-EWMA ($\lambda=0.20, K_{CS}=1.00, H_{CS}=8.74$), S²-HEWMA ($\lambda=0.20, \lambda_2=0.20, L=2.517$) (i.e. S²-DGWMA ($q=0.80, \alpha=1.00, L=2.517$)), S²-TEWMA ($\lambda=0.20, L=2.332$) and S²-GWMA ($\lambda=0.80, \alpha=0.80, L=2.8099$) charts with asymptotic control limits. The calculation details of the plotting statistics of all the considered charts are displayed in the aforementioned Table as well. Figures 1 to 7 present the S²-EWMA, S²-CUSUM, CS-EWMA, S²-HEWMA, S²-TEWMA, S²-GWMA and S²-QEWMA charts, respectively. We observe that the samples 24 to 30 raise an OOC signal in the S²-QEWMA chart, the samples 24 to 27 raise an OOC signal in the S²-TEWMA chart, while the remaining charts fail to detect the change in the process standard deviation.

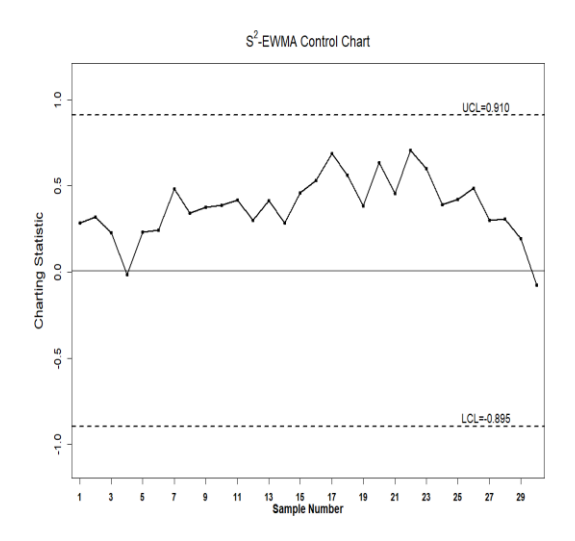


Figure 1. S²-EWMA chart with (λ , L) = (0.20, 2.8004), $ARL_0 \approx \! 370 \text{ and } n = 5$

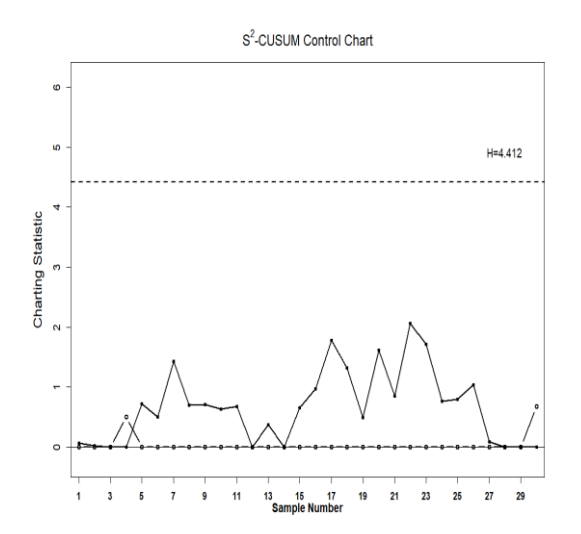


Figure 2. S²-CUSUM chart with (K, H) = (0.50, 4.412), ARL₀ ≈ 370 and n = 5

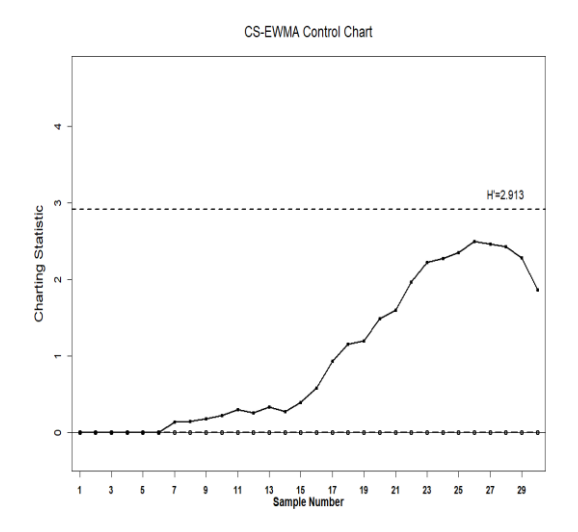


Figure 3. CS-EWMA chart with (λ , K_{CS}, H_{CS}) = (0.20, 1.00, 8.74), ARL₀ \approx 370 and n = 5

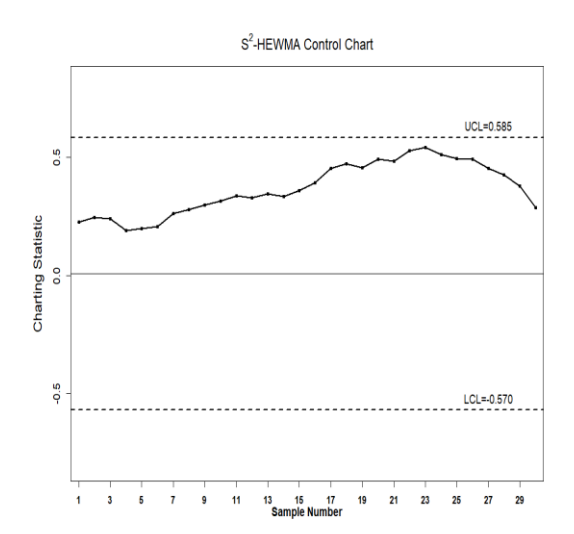


Figure 4. S²-HEWMA chart with $(\lambda_1, \lambda_2, L) = (0.20, 0.20, 2.517)$, ARL₀ ≈ 370 and n = 5

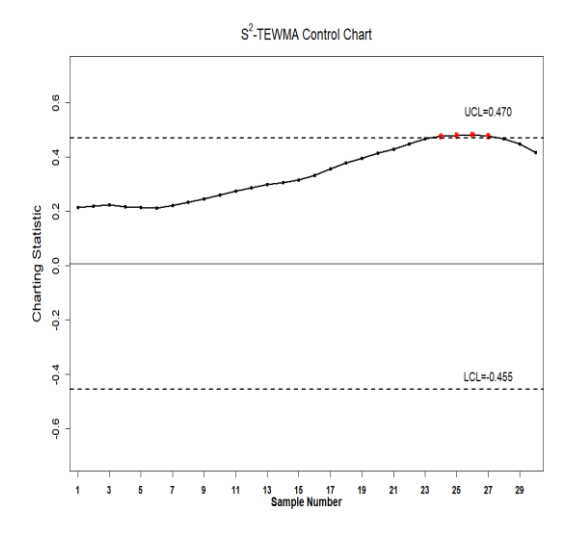


Figure 5. S²-TEWMA chart with $(\lambda, L) =$ (0.20, 2.332), ARL₀ ≈ 370 and n = 5

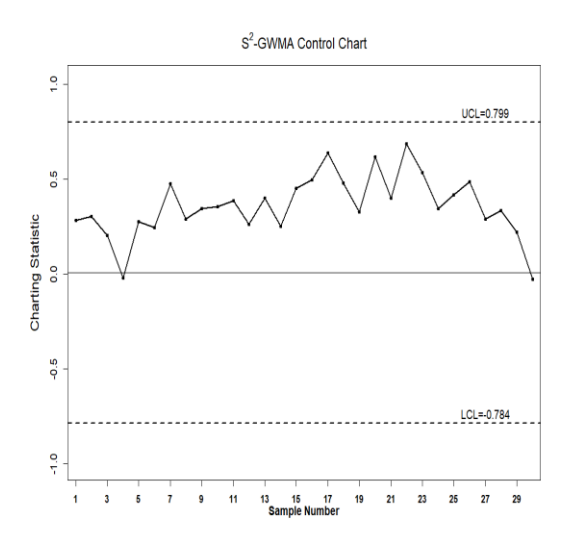


Figure 6. S²-GWMA chart with $(q, \alpha, L) =$ (0.80, 0.80, 2.8099), ARL₀ ≈ 370 and n = 5

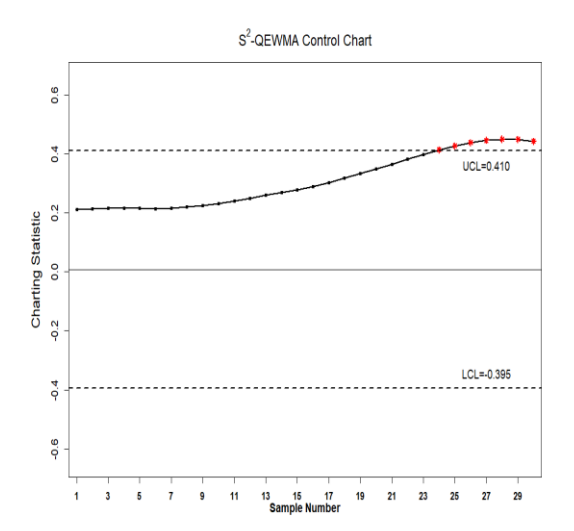


Figure 7. S²-QEWMA chart with $(\lambda, L) = (0.20, 2.2255)$, ARL₀ ≈ 370 and n = 5

6. Conclusions

In this article, we introduce a novel control chart called the S²-QEWMA chart, which utilizes a three-parameter logarithmic transformation to the sample variance, serving as an EWMA-type chart for monitoring the process dispersion. We conduct numerous Monte-Carlo simulations to determine the design parameters for the S²-QEWMA chart. Our evaluation study reveals that this chart exhibits increased sensitivity as the sample size grows. Additionally, we recommend using small λ values for detecting small deviations in the process variability, while larger λ values are more suitable for identifying moderate to large upward shifts. Furthermore, we perform a comparative analysis of the newly proposed S²-QEWMA chart against several established memory-type control charts designed for monitoring the process variability, including the S²-GWMA, S²-EWMA, S²-CUSUM, CS-EWMA, S²-HEWMA, S²-TEWMA, and S²-DGWMA

charts. The results of this comparison study indicate that the S²-QEWMA chart outperforms its competitors, especially in detecting small shifts in the process dispersion. To illustrate the implementation of our proposed chart and the aforementioned competing control charts, we provide a practical example. In future research, it would be valuable to explore the variable sampling interval version of the S²-QEWMA control chart or assess the performance of the S²-QEWMA chart under different smoothing parameters.

References

- [1] E.S. Page, "Continuous inspection schemes," Biometrika. vol. 41, pp. 100-115, 1954.
- [2] E.S. Page, "Controlling the standard deviation by CUSUMs and warning lines," *Technometrics*. vol. 5, pp. 307–315, 1963.
- [3] S.W. Roberts, "Control chart tests based on geometric moving averages," *Technometrics*. vol. 1, pp. 239–250, 1959.
- [4] S.E. Shamma, and A.K. Shamma, "Development and evaluation of control charts using double exponentially weighted moving averages," *Int. J. Qual. Reliab. Manag.* vol. 9, pp. 18–26, 1992.
- [5] L. Zhang, and G. Chen, "An extended EWMA mean chart," Qual. Technol. Quant. Manag. vol. 2, pp. 39–52, 2005.
- [6] S.H. Sheu, and T.C. Lin, "The generally weighted moving average control chart for detecting small shifts in the process mean," *Qual. Eng.* vol. 16, pp. 209–231, 2003.
- [7] A. Haq, "A new hybrid exponentially weighted moving average control chart for monitoring process mean," *Qual. Reliab. Eng. Int.* vol. 29, pp. 1015–1025, 2013.
- [8] A. Haq, "A new hybrid exponentially weighted moving average control chart for monitoring process mean: Discussion," *Qual. Reliab. Eng. Int.* vol. 33, pp. 1629–1631, 2017a.
- [9] V. Alevizakos, K. Chatterjee, and C. Koukouvinos, "The triple exponentially weighted moving average control chart," *Qual. Technol. Quant. Manag.* vol. 18, pp. 326–354, 2021.
- [10] V. Alevizakos, K. Chatterjee, and C. Koukouvinos, "The quadruple exponentially weighted moving average control chart," *Qual. Technol. Quant. Manag.* vol. 19, pp. 50–73, 2022.
- [11] P. Castagliola, "A New S²-EWMA Control Chart for Monitoring Process Variance," *Qual. Reliab. Eng. Int.* vol. 21, pp. 781–794, 2005.
- [12] P. Castagliola, G. Celano, and S. Fichera, "A New CUSUM-S² Control Chart for Monitoring the Process Variance," *J. Qual. Maint. Eng.* vol. 15, pp. 344–357, 2009.
- [13] N. Abbas, M. Riaz, and R.J.M.M. Does, "CS-EWMA Chart for Monitoring Process Dispersion, *Qual. Reliab. Eng. Int.* vol. 29, pp. 653–663, 2013.
- [14] S. Tariq, M. Noor-ul-Amin, M. Aslam, and M. Hanif, "Design of hybrid EWMln-S² control chart," *J. Ind. Prod. Eng.* vol. 36, pp. 554–562, 2019.
- [15] K. Chatterjee, C. Koukouvinos, and A. Lappa, "A new S²-TEWMA control chart for monitoring process dispersion," *Qual. Reliab. Eng. Int.* vol. 37, pp. 1334–1354, 2021.
- [16] V. Alevizakos, K. Chatterjee, C. Koukouvinos, and A. Lappa, "A double generally weighted moving average control chart for monitoring the process variability," *J. Appl. Stat.* vol. 50, pp. 2079–2107, 2023.
- [17] V. Alevizakos, K. Chatterjee, C. Koukouvinos, and A. Lappa, "A S²-GWMA control chart for monitoring the process variability," *Qual. Eng.* vol. 33, pp. 533–551, 2021.
- [18] M.R. Reynolds, and Z.G. Stoumbos, "Comparisons of some exponentially weighted moving average control charts for monitoring the process mean and variance," *Technometrics*. vol. 48, pp. 550–567, 2006.
- [19] P. Castagliola, G. Celano, S. Fichera, and F. Giuffrida, "A variable sampling interval S²-EWMA control chart for monitoring the process variance," *Int. J. Tech.Manag.* vol. 37, pp. 125–146, 2007.
- [20] P. Castagliola, G. Celano, and S. Fichera, "A Johnson's Type Transformation EWMA-S² Control Chart," *Int. J. Qual. Eng. Technol.* vol. 1, pp. 253–275, 2010.
- [21] L. Shu, and W. Jiang, "A new EWMA chart for monitoring process dispersion," *J. Qual. Technol.* vol. 40, pp. 319–331, 2008.
- [22] S.A. Abbasi, M. Riaz, A. Miller, S. Ahmad, and H.Z. Nazir, "EWMA dispersion control charts for normal and non-normal processes," *Qual. Reliab. Eng. Int.* vol. 31, pp. 1691–1704, 2015.

- [23] B. Zaman, N. Abbas, M. Riaz, and M.H. Lee, "Mixed CUSUM-EWMA chart for monitoring process dispersion," *Int. J. Adv. Manuf. Technol.* vol. 86, pp. 3025–3039, 2016.
- [24] M. Zhou, Q. Zhou, and W. Geng, "A new nonparametric control chart for monitoring variability," *Qual. Reliab. Eng. Int.* vol. 32, pp. 2471–2479, 2016.
- [25] R.A. Sanusi, M. Riaz, N. Abbas, and M.R. Abujiya, "Using FIR to Improve CUSUM Charts for Monitoring Process Dispersion," *Qual. Reliab. Eng. Int.* vol. 33, pp. 1045–1056, 2017.
- [26] R. Ali, and A. Haq, "New memory-type dispersion control charts," *Qual. Reliab. Eng. Int.* vol. 33, pp. 2131–2149, 2017.
- [27] R. Ali, and A. Haq, "New GWMA-CUSUM control chart for monitoring the process dispersion," *Qual. Reliab. Eng. Int.* vol. 34, pp. 997–1028, 2018.
- [28] A. Haq, "New EWMA control charts for monitoring process dispersion using auxiliary information," *Qual. Reliab. Eng. Int.* vol. 33, pp. 2597–2614, 2017b.
- [29] A. Haq, "A new adaptive EWMA control chart for monitoring the process dispersion," *Qual. Reliab. Eng. Int.* vol. 34, pp. 846–857, 2018.
- [30] T. Abbas, B. Zaman, A. Atir, M. Riaz, and S. Akbar Abbasi, "On improved dispersion control charts under ranked set schemes for normal and non-normal processes," *Qual. Reliab. Eng. Int.* vol. 35, pp. 1313–1341, 2019.
- [31] C.J. Huang, S.L. Lu, and J.H. Chen, "Enhanced generally weighted moving average variance charts for monitoring process variance with individual observations," *Qual. Reliab. Eng. Int.* vol. 36, pp. 285–302, 2020.
- [32] M. Riaz, S.A. Abbasi, M. Abid, and A.K. Hamzat, "A New HWMA Dispersion Control Chart with an Application to Wind Farm Data," *Mathematics*. vol. 8, 2136, 2020.
- [33] S.B. Mahadik, D.G. Godase, and W.L. Teoh, "A two-sided SPRT control chart for process dispersion," *J. Stat. Comput. Simul.* vol. 91, pp. 3603–3614, 2021.
- [34] A. Arshad, M. Noor-ul-Amin, and M. Hanif, "Function-based adaptive exponentially weighted moving average dispersion control chart," *Qual. Reliab. Eng. Int.* vol. 37, pp. 2685–2698, 2021.
- [35] A. Haq, and F. Razzaq, "New weighted adaptive CUSUM dispersion charts," *Qual. Reliab. Eng. Int.* vol. 38, pp. 110–133, 2022.
- [36] D.G. Godase, A.C. Rakitzis, S.B. Mahadik, and M.B.C. Khoo, "Deciles-based EWMA-type sign charts for process dispersion," *Qual. Reliab. Eng. Int.* vol. 38, pp. 3726–3740, 2022.
- [37] G. A. Ajibade, J. O. Ajadi, O. J. Kuboye, and E. Alih, "Generalized new exponentially weighted moving average control charts (NEWMA) for monitoring process dispersion," *Int. J. Qual. Reliab. Manag.* (2023) https://doi.org/10.1108/IJQRM- 08-2022-0257.
- [38] S.F. Yang, L.P. Chen, and C.K. Lin, "Adjustment of Measurement Error Effects on Dispersion Control Chart with Distribution-Free Quality Variable," *Sustainability*. vol. 15, 4337, 2023.
- [39] M. Jafari, M.R. Maleki, and A. Salmasnia, "A high-dimensional control chart for monitoring process variability under gauge imprecision effect," *Prod. Eng. Res. Devel.* vol. 17, pp. 547–564, 2023.
- [40] N.L. Johnson, "Systems of frequency curves generated by methods of translation," *Biometrika*. vol. 36, pp. 149–176, 1949.
- [41] N.L. Johnson, S. Kotz, N. Balakrishnan, Continuous Univariate Distributions. Wiley: New York, 1994.

Appendix

A. The following Lemma will be helpful in deriving the expectation and the variance of Q_k .

Lemma 1 For any $k \ge 1$ and $0 \le d < 1$, we have

$$\begin{split} \sum_{l=1}^k l d^{l-1} &= \left(\frac{1-d^{k+1}}{(1-d)^2}\right) - \left(\frac{(k+1)d^k}{(1-d)}\right), \\ \sum_{l=1}^k l (l-1) d^{l-2} &= -\left[\frac{k(k+1)d^{k-1}}{1-d}\right] - \left[\frac{2(k+1)d^k}{(1-d)^2}\right] + \left[\frac{2\left(1-d^{k+1}\right)}{(1-d)^3}\right], \end{split}$$

$$\begin{split} \sum_{l=1}^k l(l-1)(l-2)d^{l-3} &= -\left[\frac{k(k^2-1)d^{k-2}}{1-d}\right] - 3\left[\frac{k(k+1)d^{k-1}}{(1-d)^2}\right] - 6\left[\frac{(k+1)d^k}{(1-d)^3}\right] + 6\left[\frac{1-d^{k+1}}{(1-d)^4}\right], \\ \sum_{l=1}^k l(l-1)(l-2)(l-3)d^{l-4} &= -\left[\frac{k(k^2-1)(k-2)d^{k-3}}{1-d}\right] - 4\left[\frac{k(k^2-1)d^{k-2}}{(1-d)^2}\right] - 12\left[\frac{k(k+1)d^{k-1}}{(1-d)^3}\right] \\ -24\left[\frac{(k+1)d^k}{(1-d)^4}\right] + 24\left[\frac{1-d^{k+1}}{(1-d)^5}\right], \\ \sum_{l=1}^k l(l-1)(l-2)(l-3)(l-4)d^{l-5} &= -\frac{k(k^2-1)(k-2)(k-3)d^{k-4}}{1-d} - \frac{5k(k^2-1)(k-2)d^{k-3}}{(1-d)^2} - \frac{20k(k^2-1)d^{k-2}}{(1-d)^3} - \frac{60k(k+1)d^{k-1}}{(1-d)^4} - \frac{120(k+1)d^k}{(1-d)^5} + \frac{120(1-d^{k+1})}{(1-d)^6} \\ \sum_{l=1}^k l(l-1)(l-2)(l-3)(l-4)(l-5)d^{l-6} \\ &= -\frac{k(k^2-1)(k-2)(k-3)(k-4)d^{k-5}}{1-d} - \frac{6k(k^2-1)(k-2)(k-3)d^{k-4}}{(1-d)^2} - \frac{720(k+1)d^k}{(1-d)^6} \\ &+ \frac{30k(k^2-1)(k-2)d^{k-3}}{(1-d)^3} - \frac{120k(k^2-1)d^{k-2}}{(1-d)^4} - \frac{360k(k+1)d^{k-1}}{(1-d)^5} - \frac{720(k+1)d^k}{(1-d)^6} \\ &+ \frac{720(1-d^{k+1})}{(1-d)^7}. \end{split}$$

B. Derivation of an explicit form of Qk

Eq. (2) can be rewritten as

$$Z_{k} = \lambda \sum_{i=1}^{k} (1 - \lambda)^{k-i} T_{i} + (1 - \lambda)^{k} Z_{0}$$

$$Y_{k} = \lambda \sum_{i=1}^{k} (1 - \lambda)^{k-i} Z_{i} + (1 - \lambda)^{k} Y_{0}$$

$$W_{k} = \lambda \sum_{i=1}^{k} (1 - \lambda)^{k-i} Y_{i} + (1 - \lambda)^{k} W_{0}$$

$$Q_{k} = \lambda \sum_{i=1}^{k} (1 - \lambda)^{k-i} W_{i} + (1 - \lambda)^{k} Q_{0}$$

$$k = 1,2, ...$$
(20)

From Eq. (20), we get after algebraic simplification the following

$$Y_{k} = \lambda^{2} \sum_{i=1}^{k} (1 - \lambda)^{k-i} (k - i + 1) T_{i} + (\lambda k + 1) (1 - \lambda)^{k} Y_{0}$$

$$W_{k} = \frac{\lambda^{3}}{2} \sum_{i=1}^{k} (1 - \lambda)^{k-i} (k - i + 1) (k - i + 2) T_{i} + \left(\frac{(1 - \lambda)^{k}}{2}\right) \times \left[\lambda k (\lambda k + \lambda + 2) + 2\right] W_{0}$$

$$Q_{k} = \frac{\lambda^{4}}{6} \sum_{i=1}^{k} (1 - \lambda)^{k-i} (k - i + 1) (k - i + 2) (k - i + 3) T_{i} + \frac{(1 - \lambda)^{k}}{6} \left[\lambda k \{\lambda (k + 1) (\lambda k + 2\lambda + 3) + 6\} + 6\right] Q_{0}$$

$$(21)$$

C. Derivation of $E(Q_k)$

From Eq. (21), we get

$$E(Q_k) = \frac{\lambda^4}{6} \sum_{i=1}^k (1 - \lambda)^{k-i} (k - i + 1)(k - i + 2)(k - i + 3) E(T_i) + \frac{(1 - \lambda)^k}{6} [\lambda k \{\lambda (k + 1)(\lambda k + 2\lambda + 3) + 6\} + 6] Q_0$$

Let $d = 1 - \lambda$. Then

$$\begin{split} &\sum_{i=1}^k (1-\lambda)^{k-i}(k-i+1)(k-i+2)(k-i+3) \\ &= \sum_{u=1}^k u(u+1)(u+2)d^{u-1} = \sum_{u=1}^k u(u-1)(u-2)d^{u-1} + 6\sum_{u=1}^k u(u-1)d^{u-1} + 6\sum_{u=1}^k ud^{u-1} = 0 \end{split}$$

$$=-\frac{(k+1)(k+2)(k+3)d^k}{1-d}-\frac{3(k^2+5k+6)d^{k+1}}{(1-d)^2}-\frac{6(k+3)d^{k+2}}{(1-d)^3}-\frac{6d^{k+3}}{(1-d)^4}+\frac{6}{(1-d)^4}$$

Therefore,

$$\frac{\lambda^4}{6} \sum_{i=1}^k (1-\lambda)^{k-i} (k-i+1)(k-i+2)(k-i+3)$$

$$= -\frac{\lambda^3(k+1)(k+2)(k+3)d^k}{6} - \frac{\lambda^2(k^2+5k+6)d^{k+1}}{2} - \lambda(k+3)d^{k+2} - d^{k+3} + 1$$

Again, after simplification, we get

$$\frac{(1-\lambda)^k}{6} \left[\lambda k \{ \lambda(k+1)(\lambda k+2\lambda+3)+6 \} + 6 \right]$$

$$= \frac{\lambda^3(k+1)(k+2)(k+3)d^k}{6} + \frac{\lambda^2(k^2+5k+6)d^{k+1}}{2} + \lambda(k+3)d^{k+2} + d^{k+3}.$$

From above, it follows that

$$E(Q_k) = \mu_T(n). \tag{22}$$

D. Derivation of $Var(Q_k)$

From Eq. (21), we get

$$Var(Q_k) = \left[\frac{\lambda^8}{36} \sum_{i=1}^k (k-i+1)^2 (k-i+2)^2 (k-i+3)^2 (1-\lambda)^{2(k-i)}\right] \sigma_T^2(n).$$

Let $d = (1 - \lambda)^2$. Then

$$\begin{split} \sum_{i=1}^k (k-i+1)^2 (k-i+2)^2 (k-i+3)^2 (1-\lambda)^{2(k-i)} \\ &= \sum_{u=1}^k u^2 (u+1)^2 (u+2)^2 d^{u-1} \\ &= \sum_{u=1}^k [u(u-1)(u-2)(u-3)(u-4)(u-5) + 21u(u-1)(u-2)(u-3)(u-4) \\ &\qquad \qquad + 138u(u-1)(u-2)(u-3) + 330u(u-1)(u-2) + 252u(u-1) + 36u] d^{u-1} \\ &= \sum_{u=1}^k [u(u-1)(u-2)(u-3)(u-4)(u-5)] d^{u-1} + 21 \sum_{u=1}^k [u(u-1)(u-2)(u-3)(u-4)] d^{u-1} \\ &+ 138 \sum_{u=1}^k [u(u-1)(u-2)(u-3)] d^{u-1} + 330 \sum_{u=1}^k [u(u-1)(u-2)] d^{u-1} + 252 \sum_{u=1}^k [u(u-1)] d^{u-1} \\ &\qquad \qquad + 36 \sum_{u=1}^k u d^{u-1}. \end{split}$$

Using Lemma 1 we get, after simplification,

$$\begin{split} \sum_{i=1}^k (k-i+1)^2 (k-i+2)^2 (k-i+3)^2 (1-\lambda)^{2(k-i)} \,| \\ &= -[k(k^2-1)(k-2)(k-3)(k-4) + 21k(k^2-1)(k-2)(k-3) \\ &+ 138k(k^2-1)(k-2) + 330k(k^2-1) + 252k(k+1) + 36(k+1)] \, \frac{d^k}{1-d} \\ &- [6k(k^2-1)(k-2)(k-3) + 105k(k^2-1)(k-2) + 552k(k^2-1) + 990k(k+1) + 504(k+1) \\ &+ 36] \frac{d^{k+1}}{(1-d)^2} \\ &- [30k(k^2-1)(k-2) + 420k(k^2-1) + 1656k(k+1) + 1980(k+1) + 504] \frac{d^{k+2}}{(1-d)^3} \end{split}$$

$$\begin{split} -[120k(k^2-1) + 1260k(k+1) + 3312(k+1) + 1980] \frac{d^{k+3}}{(1-d)^4} \\ - \left[360k(k+1) + 2520(k+1) + 3312 \right] \frac{d^{k+4}}{(1-d)^5} - \left[720(k+1) + 2520 \right] \frac{d^{k+5}}{(1-d)^6} \\ - 720 \frac{d^{k+6}}{(1-d)^7} + \left[\frac{720d^5}{(1-d)^7} + \frac{2520d^4}{(1-d)^6} + \frac{3312d^3}{(1-d)^5} + \frac{1980d^2}{(1-d)^4} + \frac{504d}{(1-d)^3} + \frac{36}{(1-d)^2} \right] \end{split}$$

Therefore

$$Var(Q_k) = V(d, k)\sigma_T^2(n).$$
(23)

where

$$\begin{split} V(d,k) &= \frac{\lambda^8}{36} \big[-[k(k^2-1)(k-2)(k-3)(k-4) + 21k(k^2-1)(k-2)(k-3) + 138k(k^2-1)(k-2) + \\ &330k(k^2-1) + 252k(k+1) + 36(k+1) \big] \ \frac{d^k}{1-d} - \big[6k(k^2-1)(k-2)(k-3) + 105k(k^2-1)(k-2) \\ &+ 552k(k^2-1) + 990k(k+1) + 504(k+1) + 36 \big] \frac{d^{k+1}}{(1-d)^2} - \big[30k(k^2-1)(k-2) + 420k(k^2-1) + 1656k(k+1) + 1980(k+1) + 504 \big] \frac{d^{k+2}}{(1-d)^3} \\ &- \big[120k(k^2-1) + 1260k(k+1) + 3312(k+1) + 1980 \big] \frac{d^{k+3}}{(1-d)^4} \\ &- \big[360k(k+1) + 2520(k+1) + 3312 \big] \frac{d^{k+4}}{(1-d)^5} - \big[720(k+1) + 2520 \big] \frac{d^{k+5}}{(1-d)^6} \\ &- 720 \frac{d^{k+6}}{(1-d)^7} + \bigg[\frac{720d^5}{(1-d)^7} + \frac{2520d^4}{(1-d)^6} + \frac{3312d^3}{(1-d)^5} + \frac{1980d^2}{(1-d)^4} + \frac{504d}{(1-d)^3} + \frac{36}{(1-d)^2} \bigg] \big]. \end{split}$$

Note that, for large values of k (k $\rightarrow \infty$), the asymptotic variance of the statistic Q_k becomes

$$Var(Q_k) = V(d, \infty)\sigma_T^2(n). \tag{24}$$

where

$$V(d,k\to\infty) = \frac{\lambda^8}{36} \left[\frac{720d^5}{(1-d)^7} + \frac{2520d^4}{(1-d)^6} + \frac{3312d^3}{(1-d)^5} + \frac{1980d^2}{(1-d)^4} + \frac{504d}{(1-d)^3} + \frac{36}{(1-d)^2} \right].$$